

SPECTROSCOPIC MEASUREMENTS WITH A NEW METHOD :
THE PROJECTILE-FRAGMENTS ISOTOPIC SEPARATION

J.P. Dufour, R. Del Moral, F. Hubert, D. Jean, M.S. Pravikoff,
A. Fleury

C.E.N. Bordeaux, Le Haut Vigneau, F-33170 Gradignan, France

H. Delagrange, A.C. Mueller
GANIL, B.P. 5027, F-14021 Caen Cedex, France

K.-H. Schmidt, E. Hanelt, K. Summerer
G.S.I., D-6100 Darmstadt, Fed. Rep. of Germany

J. Frehaut, M. Beau, G. Giraudet
Commissariat à l'Energie Atomique,
Centre d'Etudes de Bruyères-le-Chatel
B.P. n° 12, F-91680 Bruyères-le-Chatel, France

ABSTRACT

A new method for the isotopic separation of projectile fragments is exposed. The application to the LISE spectrometer at GANIL provided radioactivity data on light neutron-rich nuclei (mass range 14-40). The observation on ^{17}B of the beta-delayed four neutron decay mode is reported for the first time.

INTRODUCTION

The ISOL technique has been very successful at exploiting the fragmentation of heavy nuclei by light energetic projectiles. One could however still hope to improve the Z-universality and shorten the transport times through the alternative technique of the so-called recoil spectrometers. For that purpose the inverse kinematics is highly desirable, although not strictly necessary^{1,2}. This became conceivable first at the Bevalac and then at GANIL when heavy ion beams reached the proper energy regime for projectile fragmentation. It was first shown by Symons^{2,3} that the relativistic energies allowed the use of a very simple spectrometer to identify exotic nuclei. The simplicity stemmed from the kinematics, for the fragments were forward focused in a narrow cone and had velocities very close to that of the beam. A few years ago the prospects for GANIL were more uncertain since the characteristics or even the existence of the projectile fragmentation was not clearly established below 100 MeV/n. However the beam intensity was much higher than at the Bevalac and that prompted the decision of building the LISE spectrometer. The design of the spectrometer allowed both a Time-of-Flight spectrometer mode and a new momentum-loss mode. This paper is focused on the development of this second mode and on the spectroscopic results it allowed to obtain. Other experimental results from LISE are exposed in these proceedings by D. Guillemaud-Mueller and J.C. Jacmart.

THE LISE SPECTROMETER

The originality of the device lies in its refocusing capability. As shown in fig. 1, a first section allows a momentum analysis at an intermediate focal plane and a second refocusing section provides an exit beam spot about 6 mm in diameter. The two sections also correspond to two different background environments : the target and the beam dump are separated from the experimental area by a thick concrete wall. Additional concrete has been recently added (where the dotted lines are drawn in fig. 1) to reach the very low background conditions required for neutron spectroscopy. An additional original feature of the spectrometer is the possibility to lower the magnetic rigidity of the second section so that a solid material (called here the "degrader") placed at the intermediate focal plane can slow down the ions. The purpose of this procedure is to slow down the high Z ions more than the low Z . The selection by the first dipole can thus be complemented with a further "momentum-loss" selection by the second dipole. This method, already applied to separate mono-charged elementary particles³, finds a new extension in nuclear physics which requires a charge separation as well as a mass separation. The association of the reaction mechanism properties with the momentum-loss method results in a Projectile-Fragments Isotopic Separation (PFIS). Only a summary of the properties of the PFIS method will be presented here. The very detailed characteristics of the LISE spectrometer and of the PFIS method can be found in references 4 and 5. The study of a given nucleus requires the tuning of four parameters : the target thickness, the degrader thickness, the dipole 1 magnetic rigidity ($B\rho_1$) and the dipole 2 magnetic rigidity ($B\rho_2$).

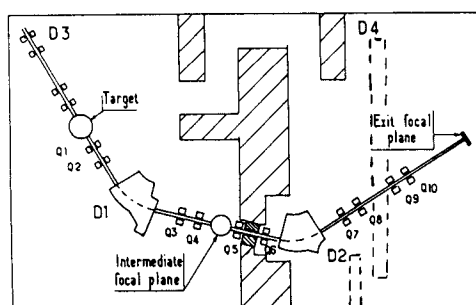


Fig. 1 : Schematic drawing of the LISE spectrometer at GANIL

The selection by the first dipole would allow a strict A/Z separation if the velocity of all the produced fragments was constant and if the target was thin. Even at intermediate energies (40-100 MeV/n), the reaction mechanism preserves the beam velocity rather well in average but a significant distribution width (close to the prediction from Goldhaber) is observed which causes a band $A/Z \pm \Delta(A/Z)$ of nuclei to be simultaneously transmitted as shown in fig. 2. In addition to this unavoidable velocity spread the target also induces a spread since the fragments formed in the first or the last matter layers do not exit the target with identical velocities. The target thickness needs to be optimized to fill the $\Delta p/p$ acceptance of

the spectrometer. The increase of the target thickness results in wider and wider projectile-fragments exit energy distributions : the total number of ions inside the accepted $\Delta p/p$ window levels off and then decreases. Typical optimum target thicknesses are 25% that of the beam range. Too large target thicknesses not only do not increase the transmitted rate but also widen the A/Z selected band through the widening of the energy distribution. The calculation of the optimum target must be made for each tuning according to the A , Z of the fragment and the opening of the slits defining the momentum acceptance.

The second selection is independent of the reaction mechanism. All the ions entering the degrader are slowed down differently according to their A , Z and also their velocity, which in turn depends on A and Z , once the $B\rho$ is fixed (v_1 (A , Z) is proportionnal to $B\rho_1 \cdot A/Z$). The $B\rho_2$ tuning can be analytically expressed as a function of $B\rho_1$, A , Z and d the degrader's thickness :

$$B\rho_2 = B\rho_1 (1 - d/R_1)^{1/2\lambda} \quad (1)$$

$$\text{with } R_1(A, Z, B\rho_1) = KB\rho_1^{2\lambda} (Z^{2\lambda-2}/A^{2\lambda-1}) \quad (2)$$

K and λ being constants depending on the stopping material only.

These formula can be easily derived with the assumption (excellent in the intermediate energy domain) that the range R of the heavy ions is proportional to $(\beta\gamma)^\lambda A/Z^2$, β and γ being the usual relativistic factors. Equation (1) shows that the ions selected at the same $B\rho_2$ are those having the same ranges R_1 (A , Z , $B\rho_1$) at the exit of the first dipole. This point illustrates for example the fact that the method can separate the A and $A+1$ isotopes having the same Z and dE/dx but different ranges. The ions not discriminated by the second selection are thus those having the same $Z^{2\lambda-2}/A^{2\lambda-1}$ ratios as shown in fig. 2.

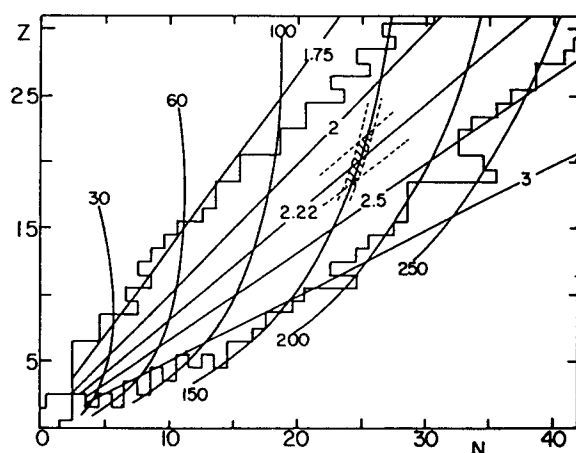


Fig. 2 : The selection operated by the degrader is shown here by a band in the N, Z plane. The lightly hatched area represents a typical selected domain which often includes only one isotope, while in less favorable cases two or three are included.

Equation (1) also leads to the determination of the shape that the degrader must have to conserve the achromatism of the line. At given distance x perpendicular to the beam axis, the magnetic rigidity is $B\rho_1(x) = B\rho_1(1+x/D_1)$ where D_1 is the dispersion of the first dipole. In order to preserve the linear dispersion, the ratio $d(x)/R_1(x)$, and also $d(x)/B\rho(x)^{2\lambda}$ must be maintained constant. One then finds that the degrader's shape must be such that :

$$d(x) = d_0 (1 + x/D_1)^{2\lambda} \quad (3)$$

It is noteworthy that this equation is independent of $B\rho_1$, $B\rho_2$, A , and Z . This "accidental" property is very useful since it allows the use of a unique degrader for several tunings on different ions. The only reasons to change the degrader are the mass and charge resolutions of the second selection which can be shown⁴⁾ to linearly scale with d/R_1 . In practice this just implied that in one experiment with a ^{40}Ar beam at 60 MeV/n, a set of three aluminium degraders (600 μ , 900 μ , 1200 μ) allowed to select a variety of ions ranging from ^{15}C to ^{40}S . The achieved resolution is shown in fig. 2 by a curved band crossing the $A/Z \pm \Delta(A/Z)$ band. The width of this second selection band can be estimated along a constant- Z cut, yielding a $(\Delta/\Delta)_A$ resolution. It must be noted that this momentum-loss resolution is very different from the usual momentum resolution of a magnet since it bears on ions all having the same initial magnetic rigidity $B\rho_1$. For degrader thicknesses going to zero, the $(\Delta/\Delta)_A$ also goes to zero and the width of the selection 2 in fig. 2 increases to infinity. In the case of LISE tuned on ^{37}P , the measured $(\Delta/\Delta)_A$ resolution reached 100 and was obtained from the ratio of the ^{37}P image diameter to the measured interval between the ^{37}P and ^{36}P images in the exit focal plane.

BETA-DELAYED GAMMA SPECTROSCOPY

Two experiments have been carried on with a ^{40}Ar beam at 60 MeV/n. The experimental detection set-up placed at the exit of LISE is shown in fig. 3.

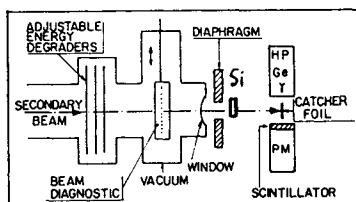


Fig. 3 : Schematic drawing of the experimental set-up placed at the exit of LISE

The detection of gammas was made by a single Ge detector (40% efficiency) in the first experiment and two NaI detectors plus a Silicon detector were added for the second experiment. The average beam intensities were 500 nA and 1 μA respectively. For the study of a given isotope the LISE tuning required less than 15 minutes and the typical data-taking time was six hours (with some exceptions !). The production rates and the nature of the measurements are listed in table 1 for the 22 studied isotopes .

Table 1 : Summary of the spectroscopic data obtained by fragmentation of a ^{40}Ar beam at GANIL. A star notes a first study, open triangles and circles respectively note improvements and confirmations of previous measurements

AZ	^{17}C	^{19}N	^{20}N	^{22}O	^{23}F	^{24}F	^{25}Ne	^{26}Ne	^{27}Na	^{30}Mg
$T_{1/2}$ (s)	0 0,20(6)	*	*	Δ 2,25(15)		*	0 0,62(3)	*	0 0,295(20)	Δ 0,342(18)
γ	*	*	*	*	Δ	*	0	*	0	0
N/s	20	>40	8	23	>200	41	510	50	>10 ³	860

^{32}Al	^{33}Al	^{34}Al	^{35}Al	^{34}Si	^{35}Si	^{36}Si	^{37}Si	^{36}P	^{37}P	^{38}P	^{40}S
Δ 0,031(6)	*	*	*	0 3,9(11)	*	*	*	0 5,35(53)	*	*	*
Δ	*	*	*	Δ	*	*	*	Δ	*	*	*
1700	260	40	5	>1600	430	100	6	22000	3300	225	58

The bulk of information gathered on these decay is very large and only part of it can be presented here. A first list of gammas, intensities and half-lives has already been published^{6,7}. The half-lives were all measured with beam pulsations uncorrelated to the nuclei implantation. The isotopes listed above lie in three different shells : p, sd and fp. The comparison of the experimental data with shell-model calculations is most complete in the sd shell where Wildenthal's predictions^{7,8} are detailed and include the β decay. The accuracy of these predictions is very impressive as can be seen in fig. 4 where the experimental over calculated half-life ratios are shown. The mean deviation \bar{X} is the one defined by Klapdor which averages the $r_{\text{max}} = \text{SUP} (T_{\text{exp}}/T_{\text{calc}} ; T_{\text{calc}}/T_{\text{exp}})$ values. In the case of ^{24}F , the ambiguity (2^+ , 3^+) in the calculation for the fundamental explains the two points placed in fig. 4.

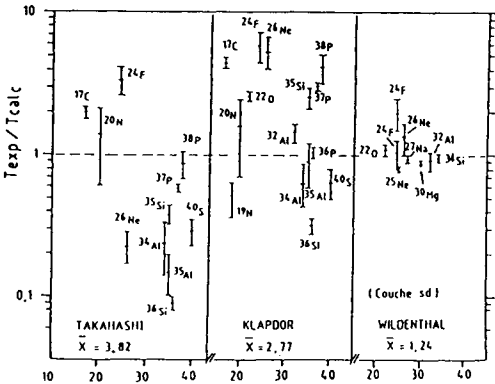


Fig. 4 : The ratios of the experimental over theoretical half-life determinations are plotted for different predictions.

Nuclei in the sd shell : an interesting property of the PFIS selection is a very good rejection rate of the daughter of the separated isotope. The beta branching of ^{23}F and ^{34}Si to the ground states of ^{23}Ne and ^{34}P have thus been obtained through the daughter's total activity determination. The experimental values ($30 \pm 8\%$ and $65.5 \pm 2.3\%$ respectively) compare well with the theoretical predictions : 33.6% and 56% . Another specificity of the apparatus is its tuning versatility and very short transport time. Those properties were especially useful in the study of ^{26}Ne . When LISE was tuned on ^{26}Ne very little gamma activity was observed in a $600\ \mu\text{s}$ beta-gamma coincidence window. The spectrometer was then tuned on ^{26}Na and it was possible to observe the direct decay of a $82.5 \pm 0.5\ \text{keV}$ excited state not in coincidence with betas. A multispectrum time-analysis starting after each implantation of a ^{26}Na isotope allowed the determination of the half-life, $9 \pm 2\ \mu\text{s}$, of this excited state. Assuming no direct feeding of the ^{26}Na ground state ($3^+ \rightarrow 0^+$ transition) leads to a decay scheme, shown in fig. 5, in good agreement with the theory.

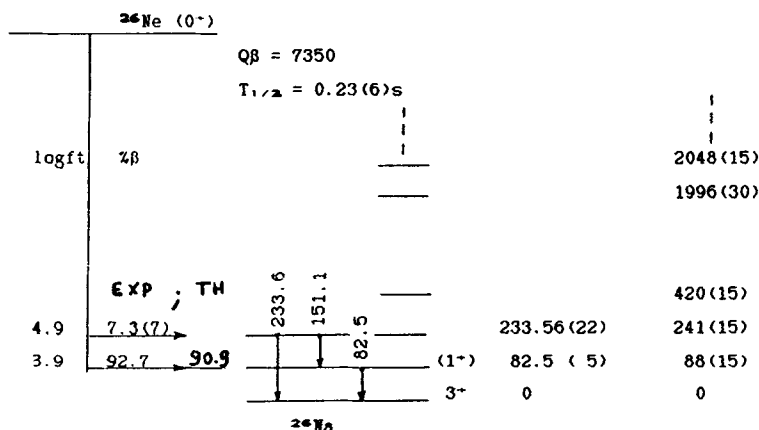


Fig. 5 : Partial decay scheme of ^{26}Ne . The half-life of the 82.5 keV level was measured $T_{1/2} = 9 \pm 2\ \mu\text{s}$

The case of ^{22}O revealed unexpected experimental difficulties. A first measurement of the half-life made by Murphy and collaborators²⁹ in 1982 yielded a value equal to $0.93 \pm 0.35\ \text{s}$. When the beam was pulsed with 2s beam-off and 2s beam-on periods, we observed an astonishingly high beam-off activity on the 637 keV main gamma-ray observed when LISE was tuned on ^{22}O . The second experiment allowed to measure the half-life of different gammas for several pulsation rates. The independent determinations all agree and converge to give an average value $T_{1/2} = 2.25 \pm 0.15\ \text{s}$, more than three standard deviations away from the 1982 value. It thus appears that the high beam-off activity first observed was due to a statistical fluctuation and not to a possible isomer. The spectroscopic data also lead to some difficulties with the observation of a strong 70.9 keV gamma ray in coincidence with the 637 keV transition. If a low energy 3^+ state (possibly at 70.9 keV) exists in ^{22}F as suggested by shell-model

calculations, then the measurements of excited states by Stokes and collaborators²⁰, or Orr¹⁰ and collaborators, are likely to have treated the 3⁺, 4⁺ doublet as one single state and that could displace their reported energies by about half the doublet width (35 keV).

Nuclei in the fp shell : the extension of the shell-model description from the sd to the fp shell, further away from the ¹⁶O inert core, has been recently improved by Warburton and Becker¹¹. The comparison

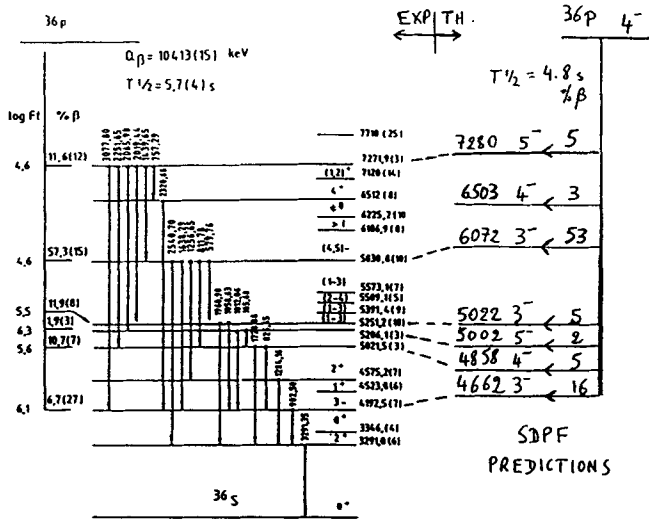


Fig.. 6 : ³⁶P decay scheme. The theoretical SDPF predictions are from ref. 11

1988DUZS placed 1994 as 4381->2386

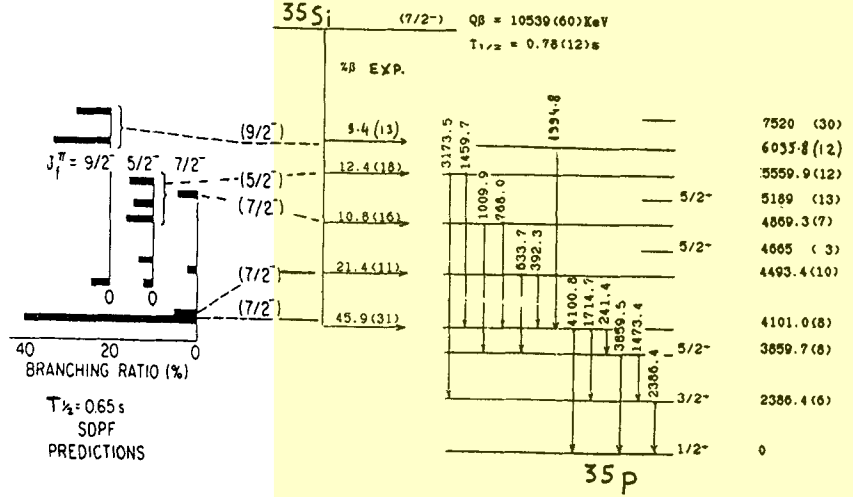


Fig. 7 : ³⁶Si decay scheme

of the experimental data with the calculation is very encouraging as can be seen in fig. 6 and 7 where the decay schemes of ^{36}P and ^{35}Si are represented. The SDPF interaction thus proves its predictive power for the $N = 21$ isotones from ^{30}Cl to ^{35}Si . Our data on ^{34}Al are still too scarce for a fruitful comparison. The experimental data need to be very extensive in this transition region where the decay from negative parity ground-states feeds very high energy excited states in the daughter. A good example is the 12% feeding from ^{36}P of the 7271 keV state in ^{36}S not seen in the first study¹²⁾ of this nucleus. Extension of these calculations is in progress for ^{37}P and ^{36}Si for which good data are available.

FIRST OBSERVATION OF THE BETA-DELAYED FOUR NEUTRON DECAY MODE

A very recent experiment was carried on with a ^{22}Ne beam at 60 MeV/n. The nuclei observed in this run are $^{17-18-19}\text{C}$, ^{17}B , ^{14}Be . The experimental set-up was designed for a maximum detection efficiency on the rare β, xn channels. The beta efficiency was improved by implanting the ions at a 2.5 mm depth in a 5 mm plastic scintillator. The photomultiplier gain was adjusted for normal beta detection while the implantation signal saturated the tube for less than 1 μs . This detector was placed in the hollow central part of a 4 π neutron detector described in ref. 13. The efficiency was measured to be 74% for neutrons at energies in the 0-3 MeV range. The identification of the nuclei separated by LISE was made with a single 300 μ thick silicon detector which provided both a ΔE and a start signal for a time of flight identification using the HF machine as a stop signal. For these light neutron-rich nuclei the PFIS separation includes essentially two isotopes of the type $A+2Z+1$, AZ . For the study of ^{17}B , ^{19}C could thus be considered as a contaminant, but due to the low counting rates and the short half-lives of these nuclei, the observed decays can easily be time-correlated to the last ^{17}B or ^{19}C implantation. The beam was stopped after any ^{17}B or ^{19}C implantation for a period of 100 ms. A target effect was clearly observed: the Be target allowed a better production of ^{18}C and ^{19}C than the Ta target whereas the opposite was true for ^{17}B . The case of ^{19}C , which is not a "pure fragmentation" product since it bears one more neutron than ^{22}Ne , seems to show that the mechanism leading to this nucleus is more of the incomplete fusion type (favored by Be) than of the deep-inelastic type (favored by Ta).

The observation of high neutron multiplicities must be accompanied by a full account of pile-up abundances, especially when using detectors with long thermalization times. With the detector used here, this average time was 11 μs and a beta-started 50 μs window allowed a full neutron collection. Another 50 μs time window was open 100 μs after the beta signal to measure the exact background conditions for each event. This procedure has been used in the metrology of neutron multiplicities in the fission process¹³⁾. The multiplicity spectra obtained for ^{17}B are shown in fig. 8.

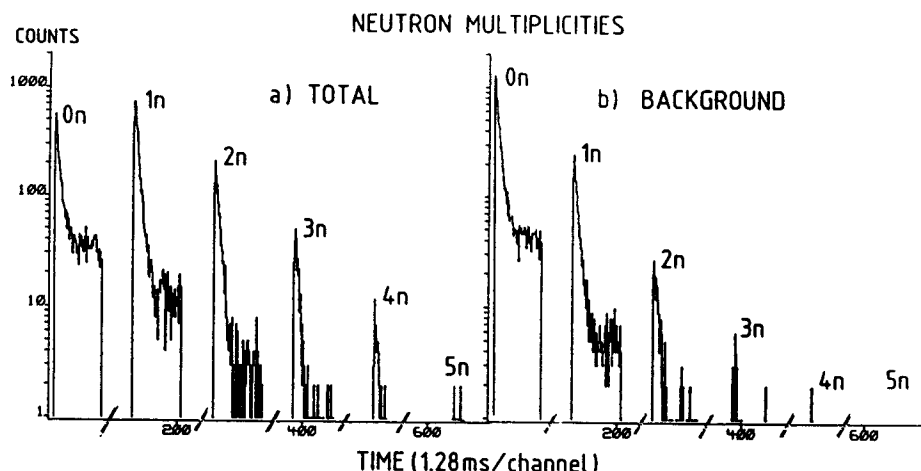


Fig. 9 : The neutron multiplicity is displayed as a function of the time difference between implantation and decay. Spectrum a) shows the data taken in a beta-coincident time window while, b) shows the data taken in a slightly decorrelated time window testing random coincidences

From these raw data two sets of corrections are made : i) the pile-up of true correlated neutrons with background events is corrected using the second coincidence window data, ii) the detection efficiency is taken into account. The measured half-lives and β , xn branchings for ^{14}Be , ^{17}B and ^{19}C are given in table 2. The observation in the case of ^{17}B of a beta-delayed four neutrons radioactivity is thus reported for the first time.

Table 2 : Preliminary beta-delayed multi-neutron branching ratios and half-lives of ^{14}Be , ^{17}B , ^{19}C

	$T_{1/2}$ (ms)	0n	1n	2n	3n	4n	Nb. events
^{14}Be	4.8(10)	0.27	0.59	0.15	$<10^{-2}$	-	2000
^{17}B	5.0(5)	0.24	0.62	0.11	$3.3 \cdot 10^{-2}$	$(4 \pm 2) \cdot 10^{-3}$	20000
^{19}C	30 (10)	-	-	-	-	-	1600

References

- 1 - J.M. WOUTERS et al. NIM A240 (1985) 77
- 2 - T.J.M. SYMONS. Phys. Rev. Lett. 42 (1979) 40
- 3 - A.P. BANFORD. "The transport of charged particle beams".
E. & F.M. Spon Ltd 1966 London p. 127
- 4 - J.P. DUFOUR et al. NIM A248 (1986) 267
- 5 - R. ANNE et al. NIM A257 (1987) 233
- 6 - J.P. DUFOUR et al. Z. Phys. A324 (1986) 487
- 7 - B.H. WILDENTHAL et al. Phys. Rev. C28 (1983) 1343
- 8 - M.J. MURPHY et al. Phys. Rev. Lett. 49 (1982) 455
- 9 - R.H. STOKES et al. Phys. Rev. 178 (1969) 1789
- 10 - N. ORR. Private communication. CANBERRA, AUSTRALIA
- 11 - E.K. Warburton et al. Phys. Rev. C34 (1986) 1031
Phys. Rev. C35 (1987) 1851
- 12 - J.C. HILL. Phys. Rev. C25 (1982) 3104
- 13 - J. FREHAUT. NIM 135 (1976) 511